Thickness Induced Structural Changes in Polystyrene Films

M. K. Mukhopadhyay,[1] X. Jiao,[2] L. B. Lurio,[3] Z. Jiang,[1,2] J. Stark,[3] M. Sprung,[2] S. Narayanan,[2] A. R. Sandy,[2] and S. K. Sinha[1]

[1]*Department of Physics, University of California San Diego, La Jolla, California 92093, USA*
[2]*Advanced Photon Source, Argonne National Laboratory, Argonne, Illinois 60439, USA*
[3]*Department of Physics, Northern Illinois University, DeKalb, Illinois 60115, USA*

(Received 5 September 2007; revised manuscript received 17 July 2008; published 10 September 2008)

Changes to the structure of polystyrene melt films as measured through the spectrum of density fluctuations have been observed as a function of film thickness down to the polymer radius of gyration (R_g). Films thicker than $4R_g$ show bulklike density fluctuations. Thinner films exhibit a peak in $S(q)$ near $q = 0$ which grows with decreasing thickness. This peak is attributed to a decreased interpenetration of chains resulting in an enhanced compressibility. Measurements were made using small angle x-ray scattering in a standing wave geometry designed to enhance scattering from the interior of the film compared to interface scattering.

DOI: 10.1103/PhysRevLett.101.115501 PACS numbers: 61.05.cf, 68.60.−p, 82.35.Gh

A fundamental question in the theory of molecular liquids is how is their structure affected by confinement on a scale comparable to the molecular size. This is particularly relevant to polymer melts since their molecular size can extend to tens of nanometers. Improved understanding of the structure of molten polymers is of technological interest for nanoscale polymeric materials. It is also of fundamental interest as a test of basic theories of polymer fluids, and to evaluate how well these theories predict structural modifications in response to perturbations which vary over molecular length scales.

Silberberg [1] advanced a hypothesis that the main effect of an interface on a polymer fluid is to reflect conformations of the polymer chains when they intersect the interface. More detailed calculations made using a range of techniques including both analytic methods [2,3] as well as Monte Carlo simulations and molecular dynamics [2–5] support Silberberg's basic conjecture. Silberberg's conjecture predicts no other change to the chain conformations. However, in films whose thickness approaches R_g reflection of a chain at an interface significantly increases the local density of the coil and thus reduces the degree of entanglement. Since the chain conformation is a function of entanglement, there must be other changes beyond Silberberg's prediction. Specifically, a reduced entanglement in thin films will make the chain conformation more like a self-avoiding random walk at short length scales relative to the random walk approximated by a bulk polymer.

Neutron experiments have tried to explore this issue by directly measuring the structure factor of an individual chain in a thin film. Some neutron experiments have observed an expansion of the chain structure [6,7], while other experiments find no change [8,9]. The conflicting results of these measurements may be due to the difficulty of separating surface from interior scattering. Some support for reduced interpenetration in thin films has also been found experimentally using other techniques. Tretinnikov *et al.* indirectly measured free volume changes in very thin films from the shift in infrared vibration bands [10]. Furthermore, free volume may play a role in the observations of a reduced glass transition temperature in thin films [11–14].

To address the shortcomings in previous work we have developed a new method using x rays to study density fluctuations in the interior of the polymer film. By setting up an x-ray standing wave within the film, scattering from the interior can be excited to the exclusion of substrate and surface scattering. We find that films thicker than $4R_g$ show density fluctuations nearly identical to the bulk, while thinner films exhibit a peak in $S(q)$ near $q = 0$ which grows with decreasing thickness, indicating an enhanced compressibility and a longer correlation length for density fluctuations. These observations are explained by reduced interpenetration of the polymer chains in thin films, resulting in a concurrent increase in free volume. We also find that the density of thin films decreases consistent with such a free volume increase. Note that x-ray scattering, unlike neutron scattering, measures collective density fluctuations rather than the structure of individual chains.

We studied polystyrene (PS) films ($M_w = 129$ K, $M_w/M_n \sim 1.05$) that were spun cast onto 20×20 mm^2 HF etched and polished silicon substrates and annealed in vacuum for 24 h at 160 °C. The thickness of the films ranged from 10 to 114 nm. The expected R_g of 129 K PS is 9.6 nm yielding a range in thickness from $1R_g$ to $12R_g$. Measurements were performed at beam line 8-ID at the Advanced Photon Source. The sample was held in a vacuum $<10^{-3}$ torr during the measurement to minimize parasitic scattering and prevent x-ray damage. The exposure was limited to 5 min to minimize damage. Data were collected over a temperature range from 50 °C to 160 °C and as a function of incident angle α from 0.13° to 0.26°.

In Fig. 1, we have schematically shown the diffuse scattering geometry. The scattered beam was collected using a CCD area detector, and the intensity was normalized to $\pm 10\%$ via a secondary standard. For each value of α a range of scattering vectors could be simultaneously measured comprising a range of in-plane scattering components from $0.5 < q_{\|} < 3$ nm^{-1} and out of plane from $0.4 < q_z < 2.3$ nm^{-1}.

Figure 2 shows the diffuse scattering as a function of α at a fixed value of total wave vector q. Two different thickness films are shown: $D = 20$ nm ($\sim 2R_g$) and 114 nm ($\sim 12R_g$). The data in each of the panels of Fig. 2 represent a combination of scattering from the surface, substrate, and the interior of the films. The effect of varying α on the intensity is particularly important over the range of angles between the critical angle for total external reflection of PS $\alpha_{c,\mathrm{PS}} \approx 0.17°$ and that of Si $\alpha_{c,\mathrm{Si}} \approx 0.24°$ at an energy 7.35 keV. In this range there is interference inside the PS film between the incident beam and the beam reflected by the Si. Some particular values of α yield a standing wave condition resulting in a single peak in Fig. 2(a) and four peaks in Fig. 2(b). At these conditions nearly all the intensity comes from the interior of the film; the surface and the substrate scattering are suppressed.

A formalism for calculating diffuse surface scattering in reflection geometry using the distorted wave Born approximation was worked out by Sinha and collaborators [15] and is described in detail by Tolan [16]. We have extended this formalism to a thin film geometry by including an integral over the electric fields throughout the film. The details of this will be presented in full in a second paper [17]. The interior scattering is then given by

$$\left.\frac{d\sigma}{d\Omega}\right|_{\text{interior}} \approx \frac{r_0^2 \rho_m f_m A_{xy}}{2\pi} S(q) Y(\alpha, \beta). \qquad (1)$$

Here α is the incident angle, β the exit angle, r_0 is the Thompson radius, ρ_m is the monomer density, A_{xy} is the illuminated surface area, $S(q)$ is the structure factor as a function of the magnitude of wave vector transfer, and $Y(\alpha, \beta)$ is an amplitude correction term that accounts for the integral of the electric field through the sample. We ignore the structure of the monomer units and take the form factor as the number of electrons $f_m = 56$. The interpretation of the scattering intensity can be further complicated by the spatial variation of the electric field in the sample; however, as long as the length scales associated with the sample structure are sufficiently distinct from the length scales associated with the electric field variation, and provided $\int S(\vec{q}) dq/q^2$ converges sufficiently fast, this effect can be neglected.

The solid lines in Fig. 2 display fits to the α dependence of the diffuse scattering where interior scattering is calculated using Eq. (1). The diffuse scattering from the interior of the film can be extracted by fitting the variation of the total diffuse scattering as a function of α with three adjustable parameters: the intensity from the surface, substrate, and the interior of the film. The intensity of the surface scattering agreed with the capillary wave theory prediction based on the temperature and the bulk surface tension [18]. Thus, the fits involved only two parameters: the intensity of the interior diffuse scattering from the film and the substrate scattering. The latter is negligible compared to the former at large $\vec{q}$, but becomes important in the small $\vec{q}$ region. We exclude data where the substrate scattering exceeds the contribution of the interior of the film at an α corresponding to the strongest peak of the standing wave inside the film. The relative contributions of surface, substrate, and interior scattering of the film are shown in Fig. 2.

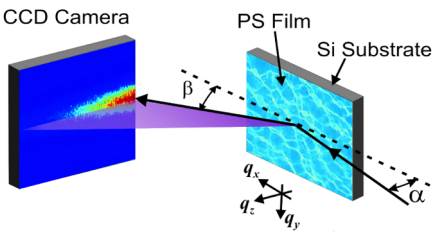

FIG. 1 (color online). Schematic of the diffuse scattering setup.

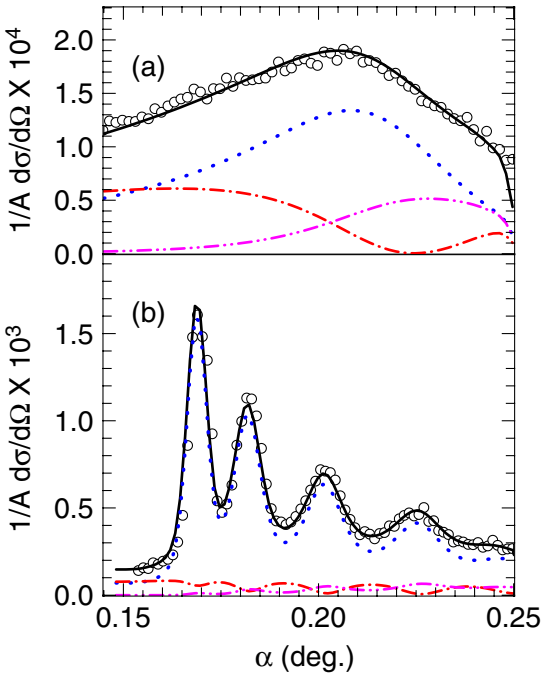

FIG. 2 (color online). Diffuse scattering cross section at $\vec{q}_{\|} = 1.525$ nm^{-1} and $q_z = 0.616$ nm^{-1} as a function of incident angle for (a) 20 nm, (b) 114 nm thick PS films on Si at 160 °C. Symbols are experimental data and the solid line is the fit. The surface (red dash-dotted line), substrate (magenta dot-dot-dashed line), and interior (blue dotted line) scattering contributions are shown separately.

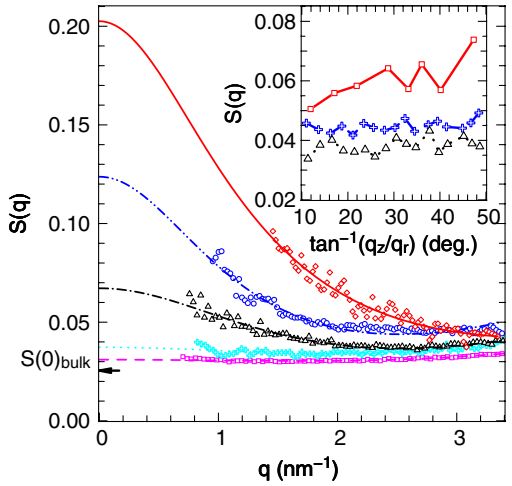

FIG. 3 (color online). $S(q)$ for film thicknesses of 10 nm (red diamonds solid line), 20 nm (blue circles dot-dot-dashed line), 38 nm (black triangles dash-dotted line), 57 nm (cyan crosses dotted line), and 105 nm (magenta squares dashed line) at 160 °C. Lines represent fits, symbols represent the measured data. The arrow marks the bulk $S(0)$. Inset: Variation of $S(q)$ with orientation at $q = 2$ nm^{-1} for film thicknesses of 10 nm (red squares solid line), 20 nm (blue crosses dashed line), and 38 nm (black triangles dotted line).

Figure 3 shows the interior contribution to $S(q)$ averaged over the orientation of $\vec{q}$. The orientation dependence of $S(\vec{q})$ at $q = 2$ nm^{-1} for various film thicknesses is shown in the inset of Fig. 3. The scattering was found to vary by around 20% with orientation in the thinnest film, with little variation in thicker films. In bulk PS the thermal diffuse scattering [19] approaches a constant at small q given by

$$S(0) = \rho_m f_m k_B T \kappa_T. \quad (2)$$

Here k_B is the Boltzmann constant, T is the temperature, and κ_T is the isothermal compressibility. For thick films Eq. (2) holds at small q and yields the expected value of κ_T. At larger q there is a rise in $S(q)$ which has also been seen previously for bulk PS by Roe and Curro [19]. They interpreted the rise as resulting from quasistatic correlations between the monomers. Roe and Curro fit their data to the form $S(q) = S(0)\exp(bq^2)$ which would also work for our thick film data, but fails for films thinner than 60 nm where there is an additional rise in intensity at small q. This behavior is qualitatively similar to the structure factor calculated in Monte Carlo simulations of thin polymer films by Binder [20], and also to the predictions of the Gaussian thread model of Schweizer and Curro [2,21].

To account for this scattering we employ a functional form inspired by the Gaussian thread model:

$$S(q) = \frac{S(0)}{1 + \xi^2 q^2} + Aq^2. \quad (3)$$

Here ξ represents a density fluctuation screening length. The Gaussian thread model [2,21] would only predict the first term in Eq. (3). The quadratic term represents the quasistatic component. This model then has three adjustable parameters, κ_T, ξ, and A. The dashed lines in Fig. 3 represent fits using this model. For brevity we focus on the data taken at $T = 160$ °C, well above T_g. Data at other temperatures above bulk $T_g \approx 100$ °C of PS are similar.

The thickness dependence of κ_T and ξ are shown in Fig. 4 for 160 °C. The compressibility shows no change for $D/R_g > 6$ and then shows a sharp increase with decreasing D up to about 7 times for the thinnest film. The thickness dependence of the compressibility can be reasonably well described by the functional form:

$$\kappa_T(D) = \kappa_T^{\text{bulk}}[1 + C_1 \exp(-D/D_0)]. \quad (4)$$

The extrapolated value of κ_T for an infinitely thick film is consistent with the bulk value. The temperature dependence of κ_T (not shown) is also consistent with that of the bulk. The values required to fit the data of compressibility as a function of thickness are $D_0 = 18.9 \pm 6.6$ nm and $C_1 = 13.6 \pm 3.8$. ξ^2 multiplied by a factor 8.0 is also plotted in the same scale to show the similar thickness dependence as compressibility.

We can qualitatively understand our results as follows. For thin films the polymer chains fold over when they reach the surface leading to a reduced entanglement. This reduced entanglement then leads to an increase in compressibility. Furthermore, as the chains become less en-

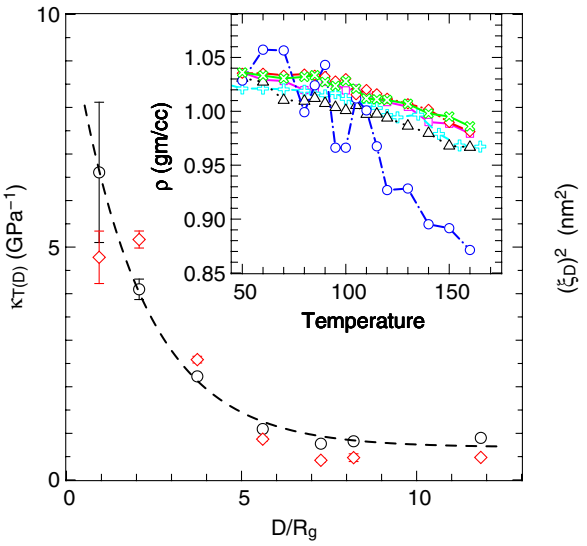

FIG. 4 (color online). Thickness dependence of fitting parameters. The black circles show the measured film compressibility. Thicknesses are normalized by the bulk radius of gyration R_g. Red diamonds show the square of the correlation length obtained from the fitting and are multiplied by a factor of 8 to appear on the same scale as the compressibility. Lines depict fits using Eq. (4). Inset: Density versus temperature for thicknesses of 20 nm (blue circles), 38 nm (black triangles), 57 nm (cyan crosses), 70 nm (red diamonds), 78 nm (green rotated crosses), and 105 nm (magenta squares).

tangled excluded volume effects become more pronounced at small length scales. This leads to a stiffening of the chains, and suppresses short length scale (but not long length scale) fluctuations leading to the observed increase in ξ. A similar mechanism was suggested by Shuto and coworkers [6] and was also recently predicted in theoretical studies by Peter *et al.* [22].

We can also understand these results in the context of the Gaussian thread model [2,21]. This model predicts that there is a relationship between κ_T and ξ given by $\kappa_T = 12(\xi/\sigma)^2/\rho k_B T$. This relation does not yield the correct value for κ_T for the known bulk statistical segment length ($\sigma \sim 0.68$ nm [9]). However the prediction that $\kappa_T \sim \xi^2$ is satisfied. This can be seen in Fig. 4.

Oyerokun and Schweizer [3] have calculated that the backfolding of polymer chains in thin films leads to an ordering of the orientation of the chains parallel to the surface. They calculate that such orientation would increase the compressibility by a factor of 3 for films with $R_g = D$. This is, however, smaller than the value found here of 7 times enhancement. This effect should be anisotropic leading to a dependence of $S(\vec{q})$ on the orientation of $\vec{q}$ with respect to the surface. This effect is seen in the present data as shown in Fig. 3.

An increase in ξ should also expand the polymer chains and consequently reduce the film density. This prediction contradicts the neutron reflectivity results of Wallace *et al.* [23], who found no change in the polymer film density with thickness. By contrast, we do find a decrease in the density for thinner films. These results are shown in the inset of Fig. 4. The decrease in the density is most apparent for thin films and only at temperatures well above T_g, which may explain the difference between our measurements and theirs.

In conclusion, we have shown that the structure factor of thin PS melt films develops a small q peak as the film thickness approaches R_g. This peak is predicted both from Monte Carlo simulations and analytic Gaussian thread calculations, and can be interpreted as the signature of an increasingly large excluded volume as characterized by an increasing correlation length ξ. Furthermore, the Gaussian thread model predicts that the compressibility should increase as the square of ξ which is also observed. While present theories qualitatively predict this result, there are no predictions which yield the correct magnitude of the observed effect nor the observed scaling with thickness. We hope that these results will motivate further development of theoretical understanding of the effects of confinement on polymer melts.

We would like to acknowledge K. Binder and K. Schweizer for useful discussions, H. Gibson for his expert technical work, and A. Habenschuss for sharing data on bulk PS melts. 'This work is supported by NSF Grant No. DMR-0209542. Use of the Advanced Photon Source at Argonne National Laboratory was supported by the U.S. Department of Energy, Office of Science, Office of Basic Energy Sciences, under Contract No. DE-AC02-06CH11357.

[1] A. Silberberg, J. Colloid Interface Sci. **90**, 86 (1982).
[2] K. S. Schweizer, in *Advances in Chemical Physics*, edited by I. Prigogine and S. A. Rice (John Wiley & Sons, New York, 1997), Vol. 98, p. 1.
[3] F. T. Oyerokun and K. S. Schweizer, J. Chem. Phys. **123**, 224901 (2005).
[4] J. Baschnagel, H. Meyer, F. Varnik, S. Metzger, M. Aichele, M. Muller, and K. Binder, Interface Sci. **11**, 159 (2003).
[5] A. Cavallo, M. Muller, J. P. Wittmer, A. Johner, and K. Binder, J. Phys. Condens. Matter **17**, S1697 (2005).
[6] K. Shuto, Y. Oishi, T. Kajiyama, and C. C. Hant, Macromolecules **26**, 6589 (1993).
[7] A. Brulet, F. Boue, A. Menelle, and J. P. Cotton, Macromolecules **33**, 997 (2000).
[8] R. L. Jones, S. K. Kumar, D. L. Ho, R. M. Briber, and T. P. Russell, Nature (London) **400**, 146 (1999).
[9] R. L. Jones, S. K. Kumar, D. L. Ho, R. M. Briber, and T. P. Russell, Macromolecules **34**, 559 (2001).
[10] O. N. Tretinnikov and R. G. Zbankov, Macromolecules **37**, 3543 (2004).
[11] J. Keddie, R. A. L. Jones, and R. A. Cory, Europhys. Lett. **27**, 59 (1994).
[12] J. A. Forrest, K. Dalnoki-Veress, J. R. Stevens, and J. R. Dutcher, Phys. Rev. Lett. **77**, 2002 (1996).
[13] J. A. Forrest, K. Dalnoki-Veress, and J. R. Dutcher, Phys. Rev. E **56**, 5705 (1997).
[14] C. J. Ellison and J. M. Torkelson, Nature Mater. **2**, 695 (2003).
[15] S. K. Sinha, E. B. Sirota, S. Garoff, and H. B. Stanley, Phys. Rev. B **38**, 2297 (1988).
[16] M. Tolan, *X-Ray Scattering from Soft-Matter Thin Films* (Springer, Berlin, 1999).
[17] M. Mukhopadhyay, Z. Jiang, S. K. Sinha, and L. B. Lurio (unpublished).
[18] L. Lurio, H. Kim, A. Ruhm, J. Basu, J. Lal, S. Sinha, and S. G. J. Mochrie, Macromolecules **36**, 5704 (2003).
[19] R. Roe and J. Curro, Macromolecules **16**, 428 (1983).
[20] K. Binder, Physica (Amsterdam) **200A**, 722 (1993).
[21] K. S. Schweizer and J. G. Curro, Chem. Phys. **149**, 105 (1990).
[22] S. Peter, H. Meyer, J. Baschnagel, and R. Seemann, J. Phys. Condens. Matter **19**, 205119 (2007),
[23] W. E. Wallace, N. C. B. Tan, W. L. Wu, and S. Satija, J. Chem. Phys. **108**, 3798 (1998).